*Korean J. Chem. Eng.*, **27**(4), 1316-1322 (2010)
DOI: 10.1007/s11814-010-0193-8

# Effect of chemical and thermal environments on structures of mesoporous silica formed in aerosol phase

**Sang Hyuk Ye and Sun-Geon Kim†**

Department of Chemical Engineering and Materials Science, Chung Ang University,
221, Huksuk-dong, Dongjak-gu, Seoul 156-756, Korea
(*Received 14 September 2009 • accepted 24 November 2009*)

**Abstract**−Spheres of mesoporous silica were prepared in aerosol phase of acidic TEOS sols having structure-directing agents (SDA) such as cetyltrimethylammonium bromide (CTAB) and Pluronic P-123. Their structural characteristics were investigated by systematically varying the chemical and thermal conditions of preparation with TEM, FT-IR, BET and SAXS. Both SDAs produced well-assembled 2-D hexagonal structures. Alcoholic solvent left better order with smaller d values than aqueous one. The upper SDA concentration for mesoporosity was much lower in the former than the latter. To get the highest order, it was important to obtain the complete self-assembly of SDA molecules without any deterioration prior to calcination. Well self-assembled mesophase appeared for the product spray dried at 100 °C and subsequently calcined at 400 °C. One-hour calcination yielded the best order. The number of domains increased with the calcination period up to 5 hrs and then decreased in further extended period. CTAB was bonded to silica surface to preserve the affinity to OH after it disappeared while P123 was not the case.

Key words: Mesoporous Silica, Structure-directing Agent, Aerosols, Nanostructures, TEOS Sols

## INTRODUCTION

Aerosol-phase self assembly has been recently demonstrated to be a continuous, rapid, simple and flexible method for synthesizing ordered mesoporous silica particles [1-4]. During a short flight of droplets having silica precursor and structure directing agents (SDA) through a heated tube, self-assembly of the SDA and sol-gel chemistry are combined to control the mesoporous structures of the particles. They have high surface area and well-organized monodisperse pores with wide applications, e.g., catalysts, electro-optical materials, controlled release agents, chromatography sorbents and adsorbents. The solvent evaporation starting at the surface of the droplet during aerosol processing induces the increase of the SDA concentration and subsequent self assembly of the SDA molecules, which grows radially inward. Unlike films showing progressive change in mesostructure by increasing the SDA concentration [1], the particles prepared with comparable CTAB concentrations showed only wormlike disordered or hexagonal mesophases, due to their curvature [1,2,5,6]. To obtain long-range order, the optimal molar ratio of CTAB to TEOS found widely varied between 0.03 and 0.25, depending on chemical and thermal environments of preparation [5-7]. Additional characteristics of the aerosol-phase preparation was that the mesophases were composed of differently oriented domains [6,8,9]. A subtle compromise has to be found between the fluidity needed for the self assembly and the rigidity needed to preserve the spherical morphology [7]. Relatively low temperatures below 150 °C were favored for the best organization from semi-solid state [5-7,10], followed by calcinations at high temperature. Lin and Bai [11] reported that pore size was uniform in the synthesized mesophase from 450 °C to 550 °C but got poorer at 650 °C.

All of these findings were obtained from precursor solutions having different compositions and aerosol reactors with different residence times and flow regimes. In addition, the optimal reactor temperature suggested was just for drying and ordering of SDA, leaving a more important step of the following pore formation accompanied by silica solidification to be elucidated. Furthermore, most researches on the optimization of preparation conditions were concentrated on CTAB only.

In this study we fixed the composition of each constituent, except SDA and solvent, in the precursor solution, reactor dimension and carrier gas flow rate. Under such condition the best ordering of the final mesophase was pursued by varying the nature and concentration of SDA, solvent composition, reactor temperature, and the temperature and time of calcination. Both CTAB and P123 were chosen as representative SDAs to study the morphology and formation mechanism of the mesophases.

## EXPERIMENTAL

The apparatus to produce mesophases consisted of ultrasonic atomizer, hot wall tubular reactor heated by an electrical furnace, filter and acid gas absorber, as shown in Fig. 1. The molar composition of precursor solution is shown in Table 1. CTAB (0.14 M) and P123 (0.09 M) were used in the same mass in the reference condition, which was chosen elsewhere [9]. Either pure water (abbreviated as "Aq") or alcoholic water (abbreviated as "Alc") was used as solvent in the same mass to see the effect of alcohol on the formation of the mesophase [4,9]. The effect of the moles of SDA per unit mole of TEOS on the morphology of the mesophase was investigated. The sols, well mixed at 30 °C, were then ultrasonically atomized at a rate of 15 mL/h. The droplets were carried by nitrogen (99.99%)

†To whom correspondence should be addressed.
E-mail: sgkim@cau.ac.kr

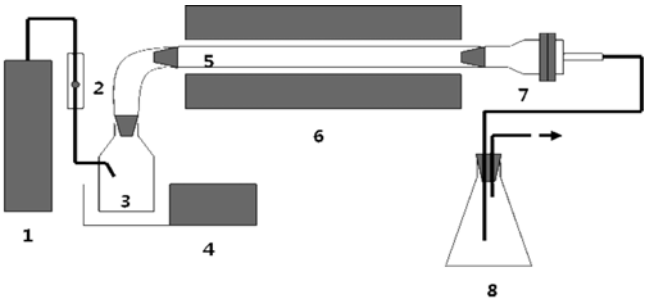


**Fig. 1. Schematic diagram of experimental apparatus.**

1. Gas
2. Flow meter
3. Precursor solution
4. Ultrasonic nebulizer
5. Reactor
6. Electrical furnace
7. Filter
8. Bubbler
9. Exit gas

**Table 1. The composition of the precursor solution used**

| | TEOS | EtOH | $H_2O$ | HCl | Structure directing agent |
|---|---|---|---|---|---|
| Aq-CTAB or P123 | 1 | 0 | 120 | 0.006 | 0.15 (CTAB) |
| Alc-CTAB | 1 | 22 | 55 | 0.004 | 0.15 |
| Alc-P123 | 1 | 22 | 55 | 0.004 | 0.009 |

flowing at 1 L/min through a horizontal tubular reactor made of quartz, 700 mm long with the diameter of 30 mm, placed in the furnace at preset temperatures. The particles exiting from the reactor were collected by the filter, while water vapor and acid formed in the reactor were absorbed in caustic solution before exhausting waste gas. The reactor set temperature was varied to see its effect on drying, organization and solidification of the mesophase. The reference reactor temperature was 400 °C.

The particles recovered from the filter, referred to "as-prepared," were further calcined at different temperatures for different times, to complete pore formation and silica solidification. The reference temperature and time of the calcination were 400 °C and 1 hr, respectively. The mesophase calcined will be called by "calcined."

**1. Characterization of Particles**

Morphologies of as-prepared and calcined mesophases were observed with scanning electron microscope (SEM, Philips 515, Philips Co.), transmission electroscope (TEM, Carl Zeiss-EM912, Omega) and high resolution transmission electron microscope (TEM, JEM4010, JEOL). Organization of pores was investigated with small angle X-ray spectroscopy (SAXS, Scintag-SDS 2000). Chemical bonds in the mesophases were identified with Fourier-transform infrared spectroscopy (FT-IR, Perkin Elmer FT-IR 1615). BET Sorptometer (ASAP 2010, Micromeritics) was used to obtain the information on specific surface area, adsorption and desorption isotherms, pore volume, pore size distribution and average pore diameter of the mesophase.

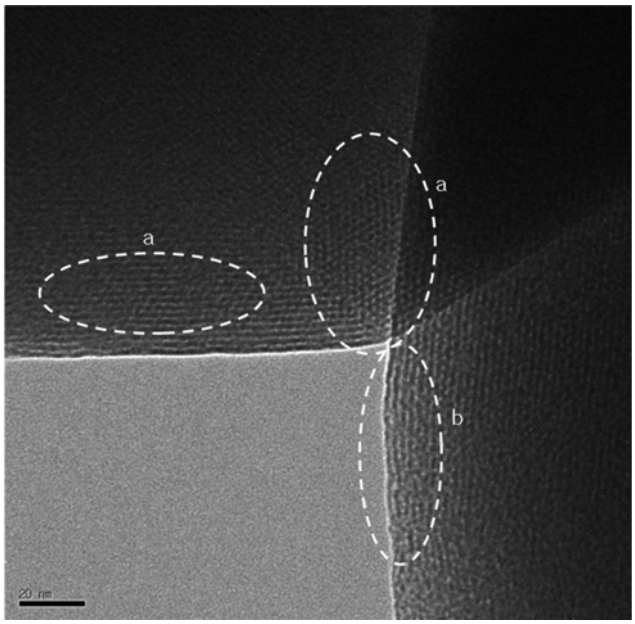


**Fig. 2. TEM images of Aq-CTAB prepared and calcined under reference condition.**

## RESULTS AND DISCUSSION

**1. Effects of Precursor Composition on Morphology of CTAB-Mesophases**

Fig. 2 shows the TEM image of Aq-CTAB prepared and calcined under reference condition. Use of CTAB resulted in 2-D hexagonal structure, some of which was oriented vertical to the image plane (designated as 'a' in the figure) and the other of which was parallel to the periphery of the sphere ('b').

The adsorption and desorption isotherms of the mesophases Alc-CTAB-0.14 and Aq-CTAB-0.28 did not have any hysteresis, while that of Aq-CTAB-0.14 did. Table 2 shows the BET specific surface area, total pore volume and average pore diameter of the three specimens. The change in the CTAB/TEOS molar ratio from 0.14 to 0.28 increased the pore volume slightly with the average pore diameter decreased, while the specific surface area increased substantially. As for Alc-CTAB-0.14, the specific surface area and pore volume were 917 $m^2/g$ and 0.6 $cm^3/g$, respectively, while the average pore diameter was 2.61 nm, smaller than that of Aq-CTAB-0.14. The adsorption-desorption isotherm of Alc-CTAB-0.14 be-

**Table 2. BET results for the mesophases prepared with CTAB**

| | CTAB (M) | BET specific surface area ($m^2/g$) | Single-point adsorption total pore volume ($cm^3/g$) | Adsorption average pore diameter (4 V/A) (nm) |
|---|---|---|---|---|
| Aq-CTAB | 0.14 | 451 | 0.336 | 3.0 |
| Aq-CTAB | 0.28 | 704 | 0.373 | 2.1 |
| Alc-CTAB | 0.14 | 917 | 0.600 | 2.61 |

longed to type IV among the six isotherm types according to the IUPAC classification, typical for the materials containing ordered mesopores. Alc-CTAB-0.14, as a type of MCM-41, had isotherms containing no hysteresis loop, due to the very narrow pore size distribution in these materials. The isotherm shape of these materials was called Type IVa [12]. Aq-CTAB-0.28 was one of type I, typical for not mesoporous but microporous materials. It also did not show any order of mesoporosity in TEM image, though not shown here. Aq-CTAB-0.14 belonged to type H2 among the four types of hysteresis loops according to the IUPAC classification, typical for materials with complex structures containing interconnected networks of pores with different size and shape.

SAXS data for Aq-CTAB and Alc-CTAB as-prepared with various CTAB concentrations are shown in Fig. 4. The peaks appearing in the figure supported that the structure of all the mesophases involved was 2-D hexagonal. The mesophase prepared from 0.035 M of CTAB had anomalously high d value, due to the incomplete assembly of the SDA molecules. Furthermore, deep SiOH band was observed in the FT-IR spectroscopy of the mesophase, indicating much pore surface of silica was not bonded to the SDA (not shown). The d values also shown in the figure decreased with the SDA concentration. Comparison of Aq-CTAB with Alc-CTAB showed that all the peak intensities of the Alc-CTAB were higher than those of the corresponding Aq-CTAB with d values and vice versa. Aq-CTAB lost their order above 0.14 M, while the order of Alc-CTAB was maintained up to 0.28 M. Therefore, it was suggested that the mesophase of Alc-CTAB was more orderly than Aq-CTAB. In the former, more volatile alcohol evaporated prior to water, saving time for the ordered texturing of CTAB, while in the latter, delayed evaporation of less volatile water deprived the time for the ordering before the TEOS-to-silica conversion. As the CTAB concentration increased above 0.14 M, which is worse, the relative amount of silica became short of filling the interstice of the 2-D hexagonal structure of CTAB, leaving Aq-CTAB-0.28 not mesoporous but microporous.

**2. Effects of Reactor Temperature on Morphology of CTAB-Mesophases**

The effect of reactor set temperature on SAXS data of Aq-CTAB and Alc-CTAB is shown in Fig. 3. The residence times in the reactor used were 13.2 s, 10.1 s, 8.2 s and 6.9 s at the reactor temperatures 400, 600, 800 and 1,000 °C, respectively. These times were too short to heat the particles exiting to the reactor set temperatures. The reac-

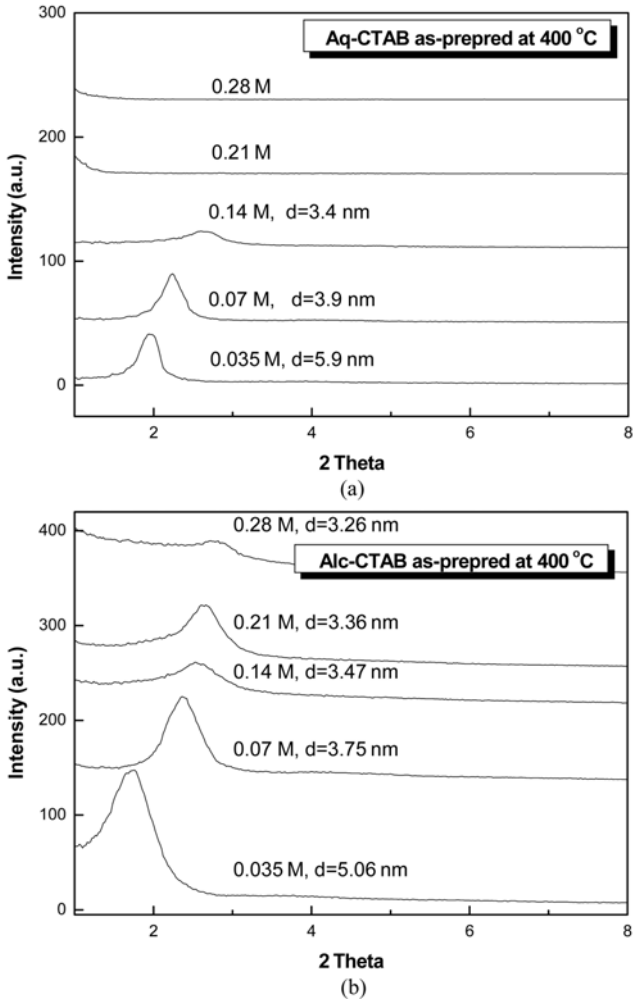


**Fig. 3. Small angle X-ray spectroscopy of (a) Aq-CTAB and (b) Alc-CTAB as-prepared, otherwise under reference condition.**

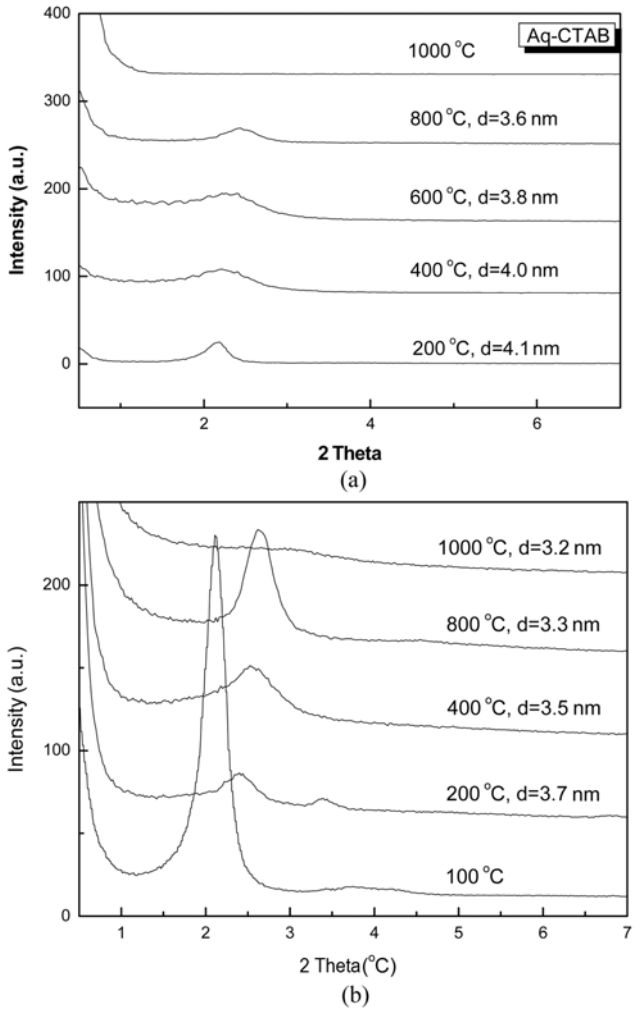


**Fig. 4. SAXS of (a) Aq-CTAB and (b) Alc-CTAB prepared at different reactor temperature otherwise under reference condition.**

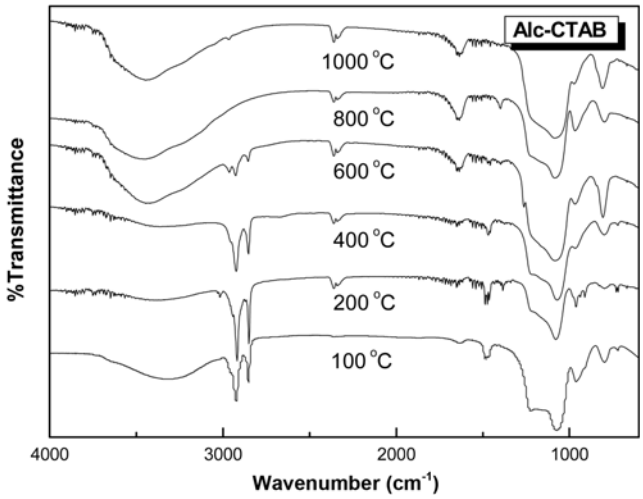


**Fig. 5. FT-IR spectra of Alc-CTAB prepared at different reactor temperature, otherwise under reference condition.**

tor temperature decreased the d value of the mesophase. At the same temperature Alc-CTAB again had higher intensity and lower d value, indicating higher order than Aq-CTAB, shown in Fig. 4. In case of Alc-CTAB, the mesophase prepared at 100 °C showed the highest intensity with the highest d value. This was explained as that the self assembly of CTAB was maximized in the half-solidified mesophase [5-8,10], as substantial amount of solvent had just evaporated. As the temperature increased above 200 °C, the intensity substantially decreased with widened peak up to 600 °C. With the increase in the reactor temperature the CTAB molecules were thermally deteriorated to disturb their assembly. The peak intensity then substantially increased at 800 °C, as all the SDA molecules were removed. Though not so clear in Aq-CTABs, a decrease in the intensity and widening in the peak up to 600 °C were also observed. Fig. 5 shows FT-IR spectra of Alc-CTAB prepared at different reactor temperatures. Though that of Aq-CTAB is not shown here, the difference in the spectroscopies was hardly found. From the figure, it was noted that the CTAB completely disappeared in 800 °C-pyrolysis. The band from 3,000 to 3,700 $cm^{-1}$ was found at 100 °C but it weakened up to 400 °C, The deep silanol (SiOH) band around 3,500 $cm^{-1}$ is clearly found for the mesophases prepared at temperatures from 600 °C to 1,000 °C. The SiOH band for 100 °C-mesophase was slightly shifted compared to those at the elevated temperatures. This suggested that CTAB molecules were bonded to the silica surface, mediated by bromide anions like in a $S^+X^-I^+$ mechanism, at 100 °C [10]. As the temperature increased above 100 °C, the CTAB molecules were chemically transformed to carbonaceous intermediates. The silica surface was covered by them until they were almost removed around 600 °C, leaving bare silica surface hydrophilic. Formation of the carbonaceous products was observed elsewhere [13] in the reaction where organics such as TEOS alcohol and/or P123 were decomposed at intermediate temperatures in nitrogen atmosphere.

### 3. Effects of Calcination on Morphology of CTAB-mesophases

While the structuring of CTAB molecules and half-solidification of the siliceous materials took place in the aerosol reactor, further treatment of calcination in air was needed to remove the SDA molecules and complete the conversion of the wall materials. Fig. 6 shows the SAXS data of Alc-CTAB prepared at 100 °C and 400 °C, respectively, followed by calcination at various temperatures, otherwise under reference conditions. The d values of all the mesophases calculated are also shown in Table 3. Better order and higher d value of as-prepared Alc-CTAB-100 than as-prepared Alc-CTAB-400 was maintained in subsequent calcination. The calcination of both the mesophases at 400 °C intensified the (100) peak showing maximum due to the complete removal of the SDA, evidenced by their FT-IR spectroscopy (not shown here). The intensity of the peak or the structural order decreased above the temperature by further silica solidification. While the peaks with higher Miller indices indicating

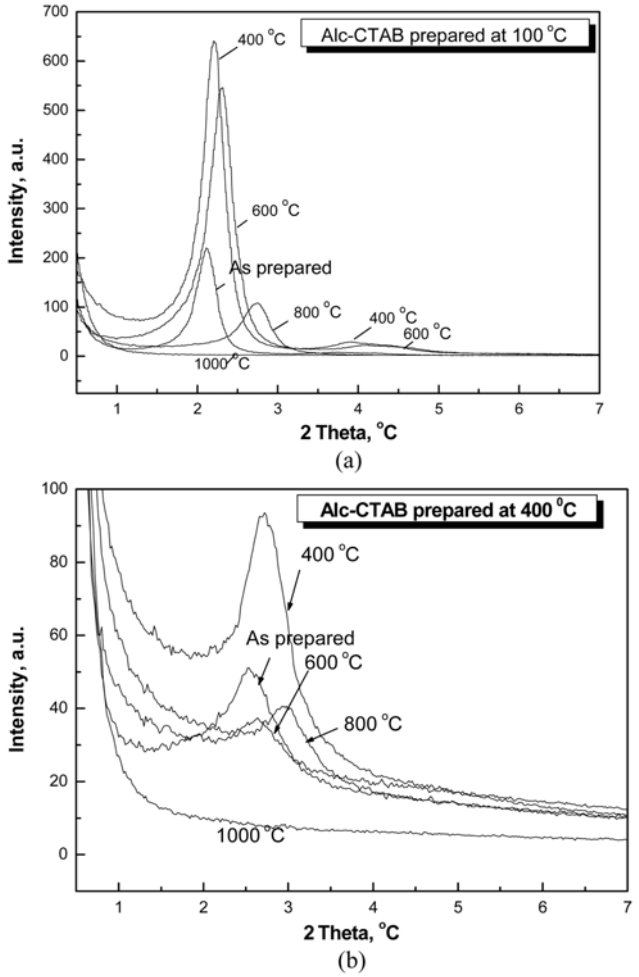


**Fig. 6. SAXS of Alc-CTABs prepared at (a) 100 °C and (b) 400 °C, respectively, and calcined at various temperatures, otherwise under reference condition.**

**Table 3. Effect of reactor temperatures (100 °C and 400 °C, respectively) on the d values of the calcined mesophases (Alc-CTAB)**

| | As prepared | 400 °C | 600 °C | 800 °C | 1,000 °C |
|---|---|---|---|---|---|
| Alc-CTAB-100 | 4.2 | 4.0 | 3.8 | 3.2 | Irregular |
| Alc-CTAB-400 | 3.5 | 3.3 | 3.3 | 3.0 | Irregular |

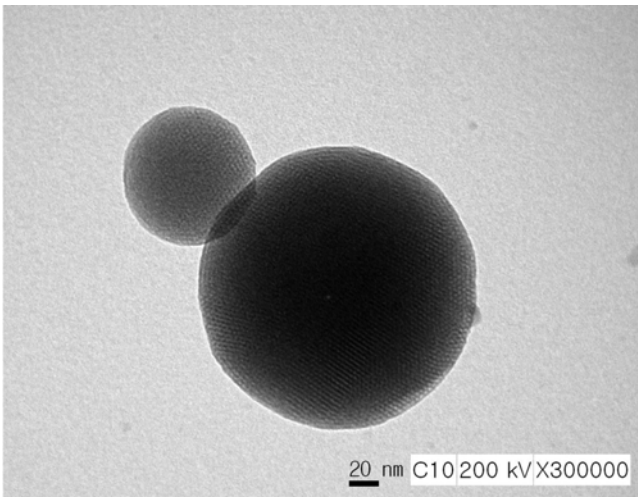


**Fig. 7. Alc-CTAB mesophase prepared at 100 °C and calcined at 500 °C for 5 hrs, otherwise under reference condition.**

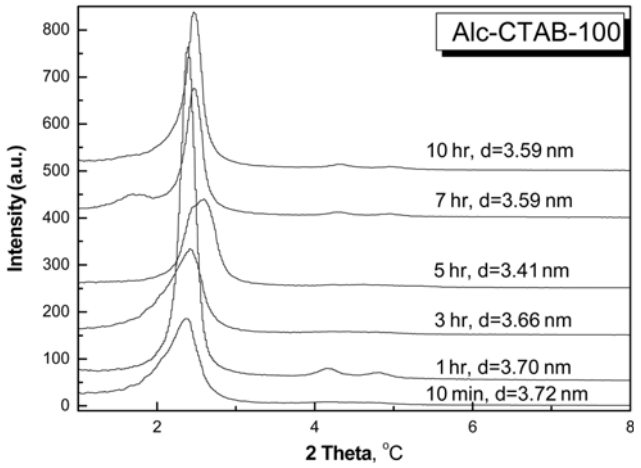


**Fig. 8. SAXS data of the Alc-CTAB-100 calcined at 500 °C for different periods.**

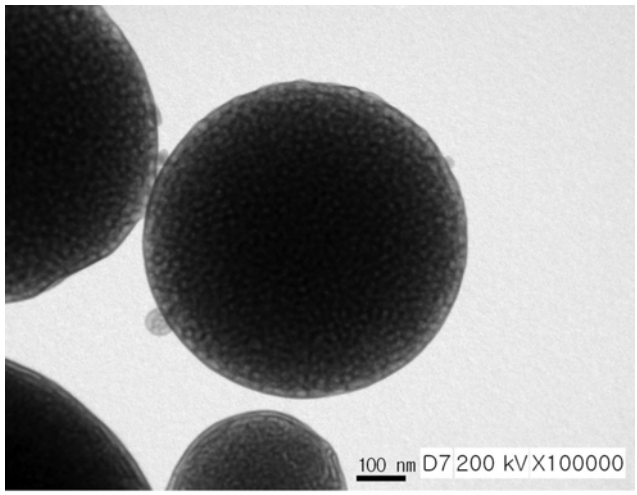


(a)

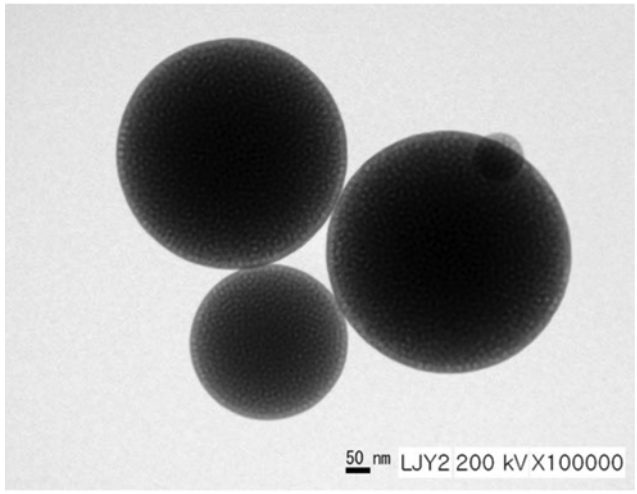


(b)

**Fig. 9. TEM image of Alc-P123 prepared with 0.0045 M (a) and calcined (b) at 400 °C for 1 hr, otherwise under reference condition.**

long-range order were undetectable except in as-prepared one in Alc-CTAB-400, they were clearly observed in all the mesophases calcined from Alc-CTAB-100. The SiOH band had maximum depth around 3,500 $cm^{-1}$ at 400 °C, which gradually decreased with the temperature to completely disappear at 1,000 °C (not shown). Fig. 7 shows the TEM image of Alc-CTAB prepared at 100 °C and then calcined for 5 hrs. The mesophase calcined for such extended period was still hexagonally oriented but composed of many multiply oriented domains. Fig. 8 shows the SAXS data of the Alc-CTAB-100 calcined at 500 °C for various periods. The mesophase calcined for one hour showed the maximum intensity or maximum order. The increase in calcination time up to 5 hrs decreased the d values and broadened the width of the peaks with their height decreasing. This indicated that the original hexagonal structures tended to differentiate into more homogeneously oriented domains. However, with further extension of the period the width and height of the (100) peak narrowed and increased, respectively, suggesting the restructuring of the mesophase took place by reducing the number of the domains. It was noted that all the mesophases calcined up to 10 hrs remained hexagonal.

## 4. The Mesophases Prepared with P123

Fig. 9 shows the TEM images of Alc-P123s prepared with 0.0045 M at 400 °C and calcined in air at 400 °C for 1hr, otherwise under reference condition. At first glance, in general, the pores in Alc-P123, also hexagonal, were substantially larger than those in Alc-CTAB. The sorption data revealed that BET specific surface area was 225 $m^2/g$ with the pore volume of 0.64 $cm^3/g$ and average pore diameter of 11.4 nm. The adsorption-desorption isotherm is shown in Fig. 10 with pore diameter distribution as inset. The isotherm showed hysteresis [14], having two steps in desorption branch as elsewhere [8]. This was supported by the peak and bump at 12 nm and 25 nm, respectively, as shown in the inset, the latter probably originating from vesicular orientation. The SAXS data of Alc-P123s prepared by varying P123 concentrations from 0.0023 to 0.18 M are shown in Fig. 11. All their (100) peaks were close to the lower limit of detection and subsequent peaks corresponding higher Miller indices were obscured by the broad and high (100) peak. The order

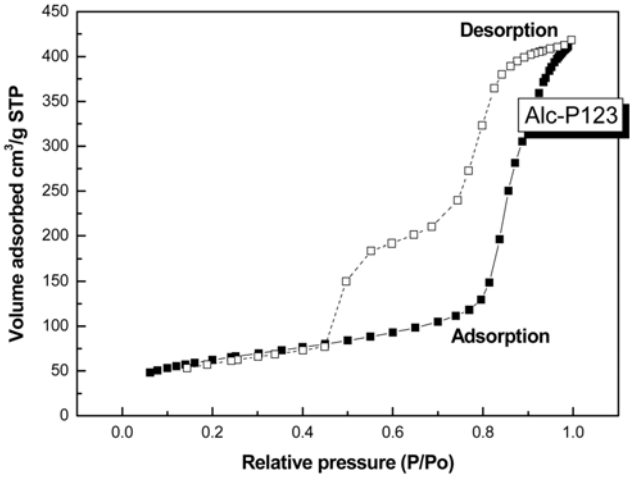


**Fig. 10. Adsorption-desorption isotherm and (Inset) pore size distribution of Alc-P123 prepared and calcined under reference condition.**

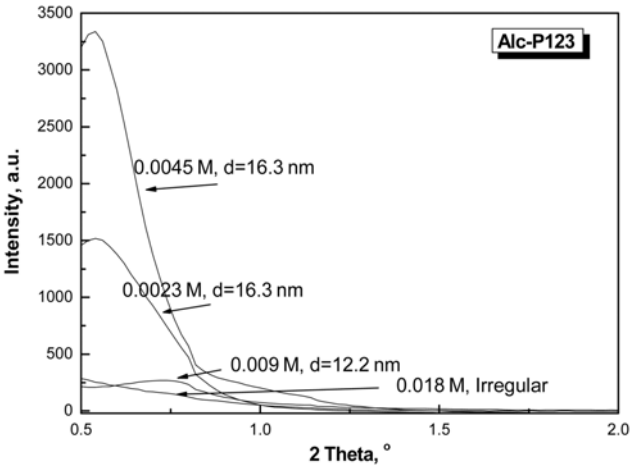


**Fig. 11. SAXS data of Alc-P123 prepared at different P123 concentrations, otherwise under reference condition.**

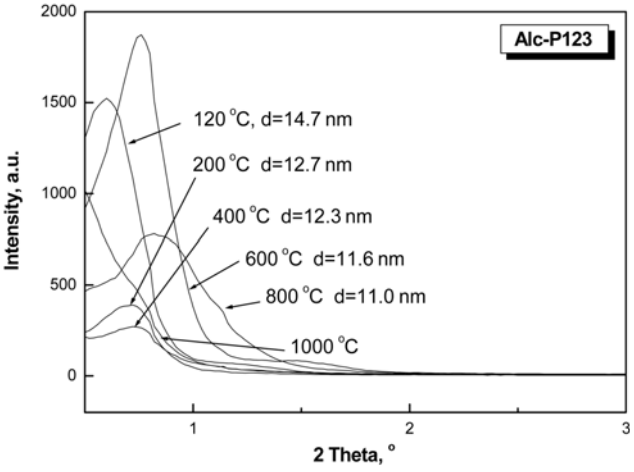


**Fig. 12. SAXS of Alc-P123 prepared at different reactor temperatures, otherwise under reference condition.**

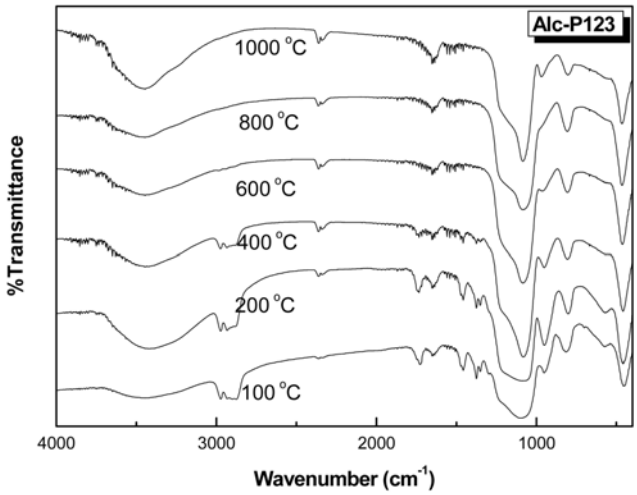


**Fig. 13. FT-IR spectra of Alc-P123 as prepared at different temperatures, otherwise under reference condition.**

was maximized with 0.0045 M P123. The SAXS data of Aq-P123, not shown here, revealed that even the (100) peak of Aq-mesophase was almost undetectable since it was shifted much closer to the lower limit of observation. This indicated that Aq-P123 also had lower order with higher d values than Alc-P123. Fig. 12 shows the SAXS data of Alc-P123 as-prepared at different reactor set temperatures. The d value monotonically decreased with the increase in the reactor set temperature. The mesophase prepared at 120 °C just after the solvent evaporation again had high order. While the preparation at higher temperatures up to 400 °C decreased the order of the mesophase, the best order including long-range ones was obtained at 600 °C. FT-IR spectra of Alc-P123 prepared at different reactor temperatures were shown in Fig. 13. By observing the $CH_2$ symmetric stretching peaks at 2,920 and 2,850 $cm^{-1}$ P123 was not observed for the mesophase prepared at 600 °C, the temperature of the SDA removal was lowered compared to CTAB. This again explained why the best order of the mesophase was obtained at the temperature. From the figure, an SiOH band around 3,500 $cm^{-1}$ was found at the temperatures as low as 120 °C and remained at temperatures up to 1,000 °C. This suggested that P123 did not bond to silica surface covalently, leaving the surface bare. Fig. 14 shows the SAXS data of the Alc-P123-100 and Alc-P123-400 calcined at different temperatures. As shown in Table 4, the d values were higher in Alc-P123-100 than Alc-P123-400 at the same calcination temperature. Once better order and higher d values were obtained as prepared, they were so at subsequent calcination, indicating the calcined mesophase structure at nonequilibrium. FT-IR spectra of Alc-P123-100 calcined at different temperatures, not shown here, showed that P123 was completely removed at 400 °C and SiOH group disappeared right above 400 °C. This was compared with the result of CTAB-based mesophases, where the SiOH group gradually faded out with the temperatures above 400 °C. As a matter of fact, since P123 was not bonded to silica surface it was removed at a lower temperature compared to CTAB not to keep the silica surface hydrophillic at elevated temperatures. The complete removal of the SDA during calcination at 400 °C left the mesophase with the best order. As with Alc-CTAB the 1-hr calcination of Alc-P123 yielded the best order and the effect

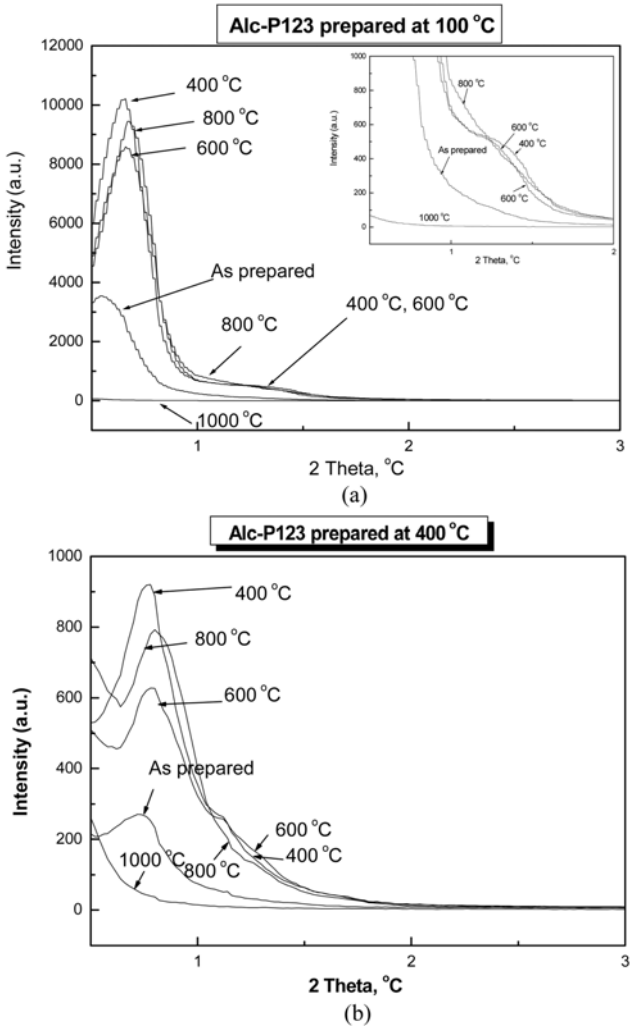


**Fig. 14. Small angle diffraction spectra of (a) Alc-P123-100 and (b) Alc-P123-400, respectively, calcined at different temperatures, otherwise under reference condition.**

**Table 4. Effect of reactor temperatures (100 °C and 400 °C, respectively) on the d values of the calcined mesophases (Alc-P123)**

| | As prepared | 400 °C | 600 °C | 800 °C | 1,000 °C |
|---|---|---|---|---|---|
| Alc-P123-100 | 16.3 | 13.4 | 13.2 | 13.4 | Irregular |
| Alc-P123-400 | 12.3 | 11.2 | 11.0 | 11.3 | Irregular |

of extended-period calcination on mesostructure was the same.

## CONCLUSION

Mesoporous silica was synthesized by spray method by varying sol composition and reactor conditions. To obtain well organized mesophases, it was important to prepare ordered assembly SDA molecules just through droplet evaporation. If the reactor temperature exceeded 100 °C to deteriorate the SDA molecules, their assembly was disturbed. When they were completely removed through the reaction at 600 °C, comparably organized mesophases were regionally obtained but not in long range. The addition of more volatile alcohol to aqueous precursors helped their assembly more ordered with smaller d values. Calcined mesophase was affected by the as-prepared state in the reactor as well calcination condition. Best organized mesophase was obtained from one-hour calcination at 400 °C of Alc-SDA-100, where all the SDA molecules were completely removed. Through calcination up to 5 hrs the mesophases were differentiated into more domains but by further extended period the phases returned back to recover the long-range order. During the extended time of calcination 2-D hexgonal structure was maintained in the mesophases. CTAB molecules helped the calcined silica surface be more hydrophilic than P123.

## ACKNOWLEDGEMENT

This research was supported by the Chung-Ang University Research Scholarship Grants in 2008.

## REFERENCES

1. C. J. Brinker, Y. Lu, A. Sellinger and H. Fan, *Adv. Mater.*, **11**, 579 (1999).
2. S. Areva, C. Boissiere, D. Grosso, T. Asakawa, C. Sanchez and M. Linden, *Chem. Commun.*, **2004**, 1630 (2004).
3. S. Rathod, G. V. R. Rao, B. Andrzejewski, G. P. Lopez, T. L. Ward, C. J. Brinker and A. K. Datye, *Mater. Res. Soc. Symp. Proc.*, **775**, 15 (2003).
4. G. Xomeritakis, C. M. Braunbarth, B. Smarsly, N. Liu, R. Kohn, Z. Klipowicz and C. J. Brinker, *Micropor. Macropor. Mat.*, **66**, 91 (2003).
5. Y. Lu, H. Fan, A. Stump, T. L. Ward, T. Rieker and C. J. Brinker, *Nature*, **398**, 223 (1999).
6. N. Baccile, D. Grosso and C. Sanchez, *J. Mater. Chem.*, **13**, 3011 (2003).
7. M. T. Bore, S. B. Rathod, T. L. Ward and A. K. Datye, *Langmuir*, **19**, 256 (2003).
8. N. Andersson, P. C. A. Alberius, J. S. Pedersen and Lennart Bergstrom, *Micropor. Mesopor. Mat.*, **72**, 175 (2004).
9. G. V. R. Rao, G. P. Lopez, J. Bravo, H. Pham, A. K., Datye, H. Xu and T. L. Ward, *Adv. Mater.*, **14**, 1301 (2002).
10. B. Alonso, A. Douy, E. Veron, J. Perez, M.-N. Rager and D. Massiot, *J. Mater. Chem.*, **14**, 2006 (2004).
11. Y.-C. Lin and H. Bai, *Aerosol. Air. Quality Res.*, **6**, 43 (2006).
12. M. D. Donohue and G. L. Aranovich, *Fluid Phase Equilibr.*, **158-160**, 557 (1999).
13. H.-S. Kim, C. S. Kim and S.-G. Kim, *J. Noncryst. Solids*, **352**, 2204 (2006).
14. Derylo-Marczewska, A. W. Marczewski, I. Skrzypek, S. Pikus and M. Kozak, *Appl. Surf. Sci.*, **252**, 625 (2005).